

# Removal of Mercury from the Environment: A Quantum-Chemical Study with the Normalized Elimination of the Small Component Method

Wenli Zou,<sup>†</sup> Michael Filatov,<sup>‡</sup> David Atwood,<sup>§</sup> and Dieter Cremer<sup>\*,†</sup>

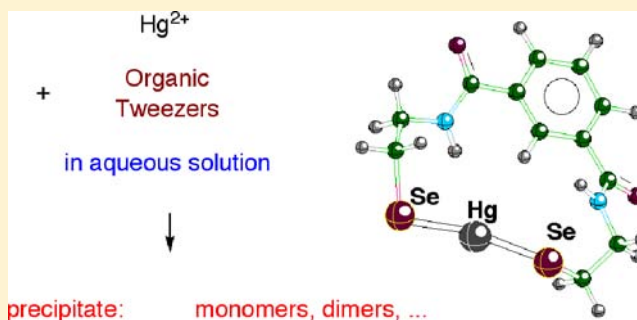
<sup>†</sup>Computational and Theoretical Chemistry Group (CATCO), Department of Chemistry, Southern Methodist University, 3215 Daniel Avenue, Dallas, Texas 75275-0314, United States

<sup>‡</sup>Mulliken Center for Theoretical Chemistry, Institut für Physikalische und Theoretische Chemie, Universität Bonn, Beringstrasse 4, D-53115 Bonn, Germany

<sup>§</sup>Department of Chemistry, University of Kentucky, Lexington, Kentucky 40506, United States

## S Supporting Information

**ABSTRACT:** 1,3-Benzenediamidoethanethiolatemercury [BDT-Hg or BD(S)-Hg] and its derivatives are investigated utilizing the Dirac exact relativistic normalized elimination of the small component method in connection with B3LYP, CCSD(T), and polarizable continuum calculations. It is shown that the chelating energy of BDT-Hg can be significantly increased by replacing sulfur with selenium or tellurium, thus leading to BD(Se)-Hg or BD(Te)-Hg. In this particular case, the chalcogenophilicity of mercury increases from S to Te because increasing the E–Hg bond lengths leads to a reduction of ring strain. Various possibilities of increasing the metal (M) chelating strength in BDT-M complexes are investigated, and suggestions for new chelating agents based on the BDT-M template are made.



## 1. INTRODUCTION

Mercury is a hazardous environmental contaminant.<sup>1,2</sup> Toxic concentrations of mercury in air, water, and soil are growing environmental threats.<sup>3</sup> They result from both natural and anthropogenic sources. Naturally occurring emissions of mercury into the atmosphere are due to volcanic eruptions, degassing from mercury mineral deposits or mercury-contaminated waters and soils, and biomass burning (e.g., forest fires).<sup>3</sup> Anthropogenic emissions mostly result from solid waste incineration, coal and oil combustion (power plants, etc.), production of gold and mercury, and pyrometallurgical processes. Atmospheric deposition of mercury leads to widespread contamination of aquatic and terrestrial ecosystems. Through biomagnification, mercury becomes available and hazardous to humans.<sup>3</sup>

Although the emission of mercury into the environment has been reduced in the last years, the mercury already emitted in previous decades, adsorbed mainly by sediment, is still dangerous for microorganisms, animals, and human beings. For mercury-contaminated aquatic systems, it may take centuries to reduce the current mercury concentrations to relatively safe mercury levels by natural self-cleaning mechanisms.<sup>3</sup> Even more pessimistic are the predictions with regard to mercury concentrations in deep sediment. To remedy this long-term problem, it will be necessary to develop nontoxic,

economical reagents that can effectively remove mercury from the environment.

Because of the problematic role of mercury for the environment, several recent investigations have focused on the detection of mercury with suitable chemical sensors.<sup>4–7</sup> Other studies have related the toxicity of mercury with its well-known chalcogenophilicity<sup>8–11</sup> and focused on the bonding of mercury to thiolates.<sup>12</sup> Despite all of the work being performed to remove mercury from the environment, there is still research on the use of mercury in solid-state nanomaterials because mercury-based quantum dots, with near-IR absorption, are easily synthesized.<sup>13</sup>

In the last 10 years, Atwood and co-workers have developed synthetic, organic, thiol-containing bidentate chelate molecules that can covalently bind mercury, cadmium, lead, and other heavy metals in aqueous solution, the compounds formed precipitate, and the precipitate can be mechanically removed from the solution.<sup>14–19</sup> BDTH<sub>2</sub> (common name, 1,3-benzenediamidoethanethiol; IUPAC name, *N,N'*-bis(2-mercaptoethyl)isophthalamide; Figure 1) has shown promise as a means of removing mercury from aqueous systems and industrial mercury-containing effluent. BDTH<sub>2</sub> has proven to be more effective than commercial reagents such as 2,4,6-

Received: November 8, 2012

Published: February 12, 2013

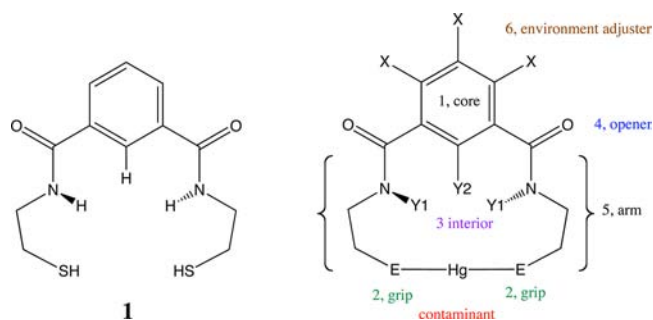


**Figure 1.** BDTH<sub>2</sub> and the BD(E)[Z]-Hg template with possible places of modification.

trimercapto-1,3,5-triazine,<sup>20</sup> sodium or potassium thiocarbonate, or sodium dimethyldithiocarbamate.<sup>21</sup>

In this work, we will investigate the binding of mercury by BDTH<sub>2</sub>, calculate the properties of BDT-Hg, and determine whether BDTH<sub>2</sub> can be improved so that it picks up mercury more effectively from aquatic systems. For the purpose of predicting how modifications of the BDT template will change the binding of mercury, we present in this work a quantum-chemical study. Relativistic effects play an important role in mercury binding,<sup>22</sup> and therefore the study was conducted with the normalized elimination of the small component (NESC) method, which corresponds to an exact relativistic two-component approach.<sup>23</sup> Recently, Zou, Filatov, and Cremer (ZFC) have developed an efficient algorithm to solve the NESC equations<sup>24</sup> and to calculate, with the help of analytical first derivatives of the NESC energy, first-order response properties such as molecular geometries,<sup>25</sup> dipole moments,<sup>25</sup> hyperfine structure constants,<sup>26</sup> electric-field gradients,<sup>27</sup> or contact densities for Mössbauer shifts.<sup>28</sup> ZFC have also developed the methodology for calculating NESC second-order response properties such as vibrational frequencies, IR intensities, or electric polarizabilities,<sup>29,30</sup> developing analytical second derivatives of the NESC energy. The NESC methodology will be used in this work to obtain reliable properties for the various BDT-Hg complexes.

The results of this work are presented in the following way. In section 2, the computational methods used in this work are described. The results of the quantum-chemical investigation of BDT-Hg complexes are presented and discussed in section 3. Conclusions will be drawn in the final section.

## 2. COMPUTATIONAL METHODS

Preliminary calculations were carried out using density functional theory with the B3LYP hybrid exchange-correlation functional,<sup>31</sup> the Stuttgart–Dresden relativistic effective core potentials (RECPs)<sup>32</sup> in connection with the def2-TZVPP<sup>33</sup> basis set for Hg (also for Mg, Zn, Br, and Te) and the 6-311G basis<sup>34</sup> for all other atoms (H, C, N, O, and F). In these calculations, the conformational flexibility of the 14-membered ring of BDT-Hg was explored. These preliminary calculations were repeated by using the NESC method as programmed by ZFC<sup>24</sup> in connection with the recontracted SARC basis set<sup>35</sup> for Zn and Hg, the Dyal’s–Dirac-contracted cc-pVTZ(fi/sf/fw) basis set for S, Mg, Se, and Br,<sup>36,37</sup> and the recontracted 6-311G basis<sup>34</sup> for all other atoms, again employing the B3LYP hybrid functional. The geometry optimizations and dipole moment calculations took advantage of the analytical NESC gradient recently published,<sup>25</sup> whereas the vibrational frequency calculations were carried out with analytical second energy derivatives for NESC.<sup>29</sup>

All NESC calculations were performed with a finite nucleus model described by a Gaussian charge distribution.<sup>38,39</sup> Furthermore,

renormalization of the one-electron Hamiltonian (*picture-change* correction) was carried out according to Liu and Peng.<sup>40</sup> For the scalar relativistic NESC approach, a velocity of light  $c = 137.035999070(98) \text{ au}$ <sup>41</sup> was used throughout the paper. In this work, only the more reliable scalar relativistic NESC, rather than any RECP results, are reported.

In another set of calculations, the NESC/B3LYP methodology was combined with the polarizable continuum model (PCM) of Tomasi and co-workers,<sup>42</sup> leading to NESC/PCM/B3LYP, which was applied to calculate BDT-Hg in aqueous solution (dielectric constant  $\epsilon = 78$ ).<sup>43</sup> Because solvation energies of cations calculated with a PCM are highly inaccurate, we used for Hg<sup>2+</sup>, Zn<sup>2+</sup>, and Mg<sup>2+</sup> the following solvation free energies taken from the literature:  $\Delta G(298, \text{solv}) = 422.1$ ,<sup>44,45</sup> 469.2,<sup>44,45</sup> and 439.2 kcal/mol.<sup>44,46</sup> In yet another set of calculations, the bond dissociation energies (BDEs) of smaller model molecules of the type M(EH)<sub>2</sub> with M = Mg, Zn, and Hg and E = S, Se, and Te were calculated with coupled-cluster theory including all single (S) and double (D) excitations and a perturbative treatment of triple (T) excitations at the CCSD(T) level of theory.<sup>47</sup> Both NESC/CCSD(T) and NESC/CCSD(T)/PCM results were obtained. In these cases, also spin–orbit coupling (SOC) effects were tested using the atomic mean-field integrals approach,<sup>48</sup> however, the effects were small, which is in line with the general understanding that SOC effects are only found for a fractional occupation of p and/or d orbitals.

For all molecules and conformations considered, the nature of the stationary states investigated was verified by frequency calculations. Vibrational, thermochemical, and entropical corrections were also determined to report, besides energy differences  $\Delta E$ , free energy differences  $\Delta G(298)$  at 298 K. In some cases, a geometry optimization at C<sub>1</sub> symmetry led to somewhat lower energies. However, if the frequency calculation at the higher symmetry yielded imaginary frequencies lower than 50i cm<sup>-1</sup>, the higher symmetry form was taken nevertheless. We use abbreviations BDT-M (E = S; M = metal), BD(E)-M [E stands for a chalcogen where “E” is used to avoid confusion with BDE], and BD(E)[Z]-M [Z-substituted BD(E)-M, where Z will be specified in the following section] to identify the molecules investigated in a short but concise form. For all geometries calculated [in total 34 BD(E)-M forms plus molecules M(EH)<sub>2</sub>, HE-M<sup>+</sup>, and HE<sup>-</sup>], NESC dipole moments<sup>25</sup> were determined and a natural bond orbital (NBO) analysis<sup>49–51</sup> was carried out in the gas phase and aqueous solution to determine the charge distribution in each molecule.

Beside the BDT-Hg compounds, we investigated also 1,3-benzenediamidoethaneselenolatemercury, BD(Se)-Hg, and the corresponding tellurolatemercury compound, BD(Te)-Hg. All optimized geometries, corresponding energies and free energies, dipole moments, and NBO charges of M(EH)<sub>2</sub>, HE-M<sup>+</sup>, and HE<sup>-</sup> are listed in the Supporting Information.

## 3. RESULTS AND DISCUSSION

BDTH<sub>2</sub> (**1** in Figure 1) is normally used in the form of its sodium thiolate to react with mercury ions, Hg<sup>2+</sup>, thus yielding BDT-Hg.<sup>14–19</sup> In Figure 1, the covalently bonded BDT-Hg molecule is also given in the form of a generalized template to differentiate between various positions in the BD(E) body and to investigate possibilities of improving the primary functionality of the BD(E) part, namely, to chelate mercury ions.

The essential features of the BD(E) template are core (1), (tweezers) arms (5), and grip (2) (see Figure 1). In the work of Atwood and his group,<sup>14–19</sup> it has been clarified that the combination of a benzene core, arms stabilized by amide groups to reduce their flexibility, and a covalent grip provided by two thiolate groups gives the molecule the ability of capturing mercury and other metal ions from aqueous solution. Therefore, the computer-assisted design will start from these results. Modifications must lead to fulfillment of the following requirements:

(1) Bonding by the tweezers molecule must be so effective in aqueous solution that ppb concentrations of the contaminant can be removed. (2) Bonding of the contaminant must be so specific that noncontaminants (metal ions such as Ca and Mg) do not neutralize the cleaner. (3) Despite the fact that the cleaner is based on an organic core, it should have a reasonable solubility in water. (4) The cleaner compound must be environmentally friendly, which implies that it is nontoxic and stable and does not lead to unwanted degradation products. (5) Excess cleaner must be easily removed from waters (rivers, lakes, surface, and ground waters). (6) It must be possible to synthesize the target compound in an easy and economic way, which is an essential prerequisite for keeping the large-scale production costs as low as possible.

For this purpose, we will investigate (i) whether the reference system should be BDT-Na<sub>2</sub> as in the experiments or some other system of the type BD(E)-M, where M is a metal cation of the type M<sup>2+</sup>, which can be easily replaced by Hg<sup>2+</sup>, (ii) whether the chelating ion S<sup>-</sup> (the grip) can be replaced by more effective chelating functionalities, (iii) whether binding of Hg can be enhanced by replacing one of the internal H atoms (Y = H; Figure 1) by other atoms with through-space interaction possibilities, (iv) whether the core can be modified in such a way as to increase mercury binding, and (v) whether the hydrophilic part of the organic tweezers can be changed in such a way that the water solubility of the starting compound is enhanced. Before considering these questions, we discuss the results obtained for the prototypical molecule BDT-Hg.

**Structure and Conformation of BDT-Hg.** The most stable conformation of BDT-Hg has C<sub>2</sub> symmetry (Figure 2).

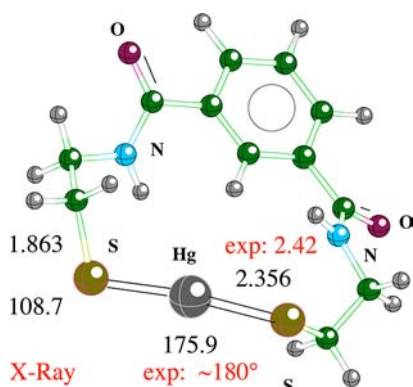


**Figure 2.** NESC/B3LYP geometry of BDT-Hg. Distances in angstroms and angles in degrees.

The benzene ring and its substituents are in a plane, with all deviations from this plane being smaller than 3° according to calculated dihedral angles. The amido groups are rotated by 31° out of the benzene plane so that one keto group points downward and the other upward.  $\pi$  delocalization between benzene and the amido groups is interrupted by this rotation, as is reflected by the length of the linking C–C bonds: 1.497 Å, which is typical of the central butadiene C–C bond for a 90°-rotated form, i.e., a C(sp<sup>2</sup>)–C(sp<sup>2</sup>) bond length without  $\pi$  delocalization.<sup>52,53</sup>

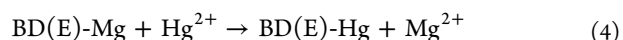
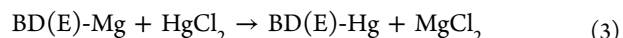
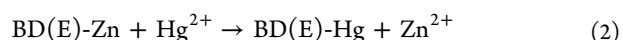
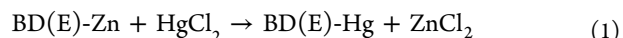
The driving force for puckering of the 14-membered ring is the strong repulsion between the benzene H atom in the Y2 position and the (N)-H atoms in the Y1 position (see Figure 1). In the puckered form, the H(Y1) and H(Y2) atoms are still 2.155 Å apart, which is somewhat smaller than the H–H van

der Waals distance. The methylene groups are perfectly staggered; however, the angle bending strain building up at the S atoms (the C–S–Hg angle is widened to 106.5°) can only be reduced by a slight inward movement of the Hg atom (S–Hg–S angle = 175.8°) away from the ideal linear arrangement. The closest Hg···H contact [with H(Y2); see Figure 1] is 3.310 Å, which is well beyond the sum of the van der Waals radii of Hg (1.55 Å<sup>54</sup>) and H (1.2 Å<sup>43</sup>). The interactions between the Hg and interior H atoms are all repulsive because all of them are positively charged.

The C<sub>s</sub>-symmetrical forms of BDT-Hg corresponding to long-chain forms (the two N atoms and the C atoms of the methylene groups are in one plane) of the 14-membered ring are higher in energy, with the lowest of these being 3.57 kcal/mol less stable (free energy difference = 4.07 kcal/mol). The higher energy is a result of increasing strain. The methylene groups try to adopt a staggered conformation with the result that (i) the C=O–N–H units are no longer in a plane (15.5° deviation) and (ii) the C–S–Hg angle is widened to 110.4°, although S prefers bond angles in the range 92–94° (see below). The angle of 110.4° is only possible due to an inward bending of the S–Hg–S unit (bending angle 166.5°). Replacement of Hg with Zn or Mg does not lead to a reduction of this energy difference, and therefore all other BDT-M forms were investigated with a C<sub>2</sub>-symmetry constraint.

**Choice of the Reference System.** We define a water-soluble reference system of the type BDT-M as one in which M is easily replaced by Hg ions. This implies that the chalcogenophilicity of M is lower than that of Hg. We define the term chalcogenophilicity as the heterolytic binding affinity of M<sup>2+</sup> ions (relative to that of suitable reference ions R<sup>2+</sup>) to chalcogen anions in the gas phase to consider just the electronic effects. Of course, the binding affinity must also be considered in aqueous solution, where factors such as the solvation energies of the ions may play a role. Hence, the chalcogenophilicity of mercury must always be specified by giving the oxidation state of mercury, its coordination number, the environment, and the reference ion R<sup>2+</sup>.

All experimental work has so far been carried out with BDT-Na<sub>2</sub> as a reference (R<sup>2+</sup> = Na<sup>+</sup>), i.e., as a starting agent of the mercury precipitation process in aqueous solution.<sup>14–19</sup> In this work, we have investigated two possibilities of a suitable reference metal ion R<sup>2+</sup>. The first concerns the group 12 homologue Zn because it should have binding properties similar to but, as a borderline Lewis acid, slightly lower than those of chalcogen S compared to Hg. It has been experimentally demonstrated that Hg<sup>2+</sup> will replace Zn<sup>2+</sup> in BDT-Zn to form BDT-Hg.<sup>17</sup> The second possible reference R<sup>2+</sup> that was tested is Mg<sup>2+</sup> for reasons to be discussed below. The suitability of these metal ions was investigated by calculating the reaction energies  $\Delta E$  and reaction free energies  $\Delta G(298)$  of reactions 1–4 both in the gas phase and in aqueous solution:



In each case, the reaction partner is either HgCl<sub>2</sub> or Hg<sup>2+</sup>. By considering the energetics of 1 (3) and 2 (4), the solvation

**Table 1.** NESC/B3LYP and NESC/PCM/B3LYP Energies  $\Delta E$  and Free Energies  $\Delta G(298)$  (All in kcal/mol) of Reactions 1–4 involving BD(E)-M

	BDT-M, Where M = Zn							
	reaction 1				reaction 2			
	$\Delta E$		$\Delta G(298)$		$\Delta E$		$\Delta G(298)$	
	gas	water	gas	water	gas	water	gas	water
E = S	-14.1	-9.5	-14.1	-9.2	-2.1	-58.0	-3.2	-58.1
E = Se	-17.7	-12.6	-17.6	-13.5	-5.6	-61.0	-6.7	-62.4
E = Te	-22.2	-17.0	-22.1	-18.6	-10.1	-65.4	-11.2	-67.5

	BDT-M, Where M = Mg							
	reaction 3				reaction 4			
	$\Delta E$		$\Delta G(298)$		$\Delta E$		$\Delta G(298)$	
	gas	water	gas	water	gas	water	gas	water
E = S	-31.2	-25.6	-30.8	-25.7	-98.0	-110.3	-99.2	-111.9
E = Se	-36.5	-30.8	-36.2	-30.1	-103.4	-115.5	-104.6	-116.3
E = Te	-44.7	-38.1	-44.7	-38.3	-111.6	-122.9	-113.1	-124.5

effects can be separated from the electronic effects. The energies obtained at the NESC/B3LYP and NESC/PCM/B3LYP levels of theory are summarized in Table 1.

According to the energies given in Table 1, BDT-Zn has bonding properties similar to those of BDT-Hg, thus leading for reaction 2 in the gas phase to small exothermic reaction energies. This changes in solution because of the more than 45 kcal/mol larger solvation energy of the  $Zn^{2+}$  ion in aqueous solution ( $-469.2$  kcal/mol<sup>44,45</sup>) compared to that of the  $Hg^{2+}$  cation ( $-422.1$  kcal/mol<sup>44,45</sup>). The exothermicity of reaction 2 increases to  $-58$  kcal/mol (Table 1). We note in this connection that the dipole moment of BDT-Zn is just 3.30 D, whereas that of BDT-Hg is 7.54 D, which implies that the latter molecule is better solvated, thus adding to the exothermicity of reaction 2 in aqueous solution. However, this exothermicity would be considerably lower ( $-9$  kcal/mol) if undissociated mercury and zinc dichloride would be involved. Considering that a high concentration of  $Zn^{2+}$  ions in solution is highly toxic to plants, invertebrates, and even vertebrate fish,<sup>55</sup> we refrain from using BDT-Zn as a reference and instead choose BDT-Mg.

Mg has an electron configuration similar to that of Hg ( $ns^2$ ); however, it does not establish as strong bonds to S as Hg does (see below). The energetics of reactions 3 and 4 are all strongly exothermic (see Table 1). The solvation energy of the  $Mg^{2+}$  ion ( $-439.2$  kcal/mol<sup>44,46</sup>) is 17 kcal/mol larger than that of  $Hg^{2+}$  and the dipole moment of BDT-Mg (3.34 D) comparable to that of BDT-Zn. Because the introduction of extra  $Mg^{2+}$  ions does not lead to any environmental problems, we have chosen BDT-Mg rather than BDT- $Na_2^{14-19}$  as a suitable starting reagent for reaction with Hg ions.

**Improving the Grip.** The largest HgEH and Hg(EH)<sub>2</sub> BDEs are found for S.<sup>8,22</sup> In this work, we want to investigate the Hg–E bonding in BDT-Hg, i.e., dicoordinated Hg of oxidation state II both in the gas phase and in solution. For this purpose, we have carried out high-level ab initio calculations for the reference system utilizing NESC/CCSD(T) methodology. The results of these calculations are summarized in Table 2.

**Table 2.** NESC/CCSD(T) and NESC/PCM/CCSD(T) Energies  $\Delta E$  (All in kcal/mol) of Dissociation Reactions 5–8

	M = Mg		
	$\Delta E$		
	reaction 5		reaction 6
	gas	water	gas
E = S	207.4	29.6	81.0
E = Se	196.4	25.2	75.4
E = Te	192.0	29.5	67.5

	M = Hg		
	$\Delta E$		
	reaction 7		reaction 8
	gas	water	gas
E = S	220.9	43.3	67.7
E = Se	208.6	39.4	62.6
E = Te	205.3	46.9	60.2



All calculated E–M–E units are linear, whereas the M–E–H angles decrease from  $94.5^\circ$  (S) to  $92.1^\circ$  (Se) to  $90.7^\circ$  (Te), which is a result of the second-order Jahn–Teller effect active in EA<sub>2</sub> systems [e.g., the H–E–H angle decreases with increasing electropositivity (atomic number) of E]. The H–E–E–H dihedral angle is always close to  $135^\circ$ , as a result of electron lone-pair staggering. The calculated heterolytic BDEs reveal that (i) the Hg–E bond strength of  $Hg^{II}$  is clearly higher for S (220.9 kcal/mol; Table 2) than Se (208.6) or Te (204 kcal/mol) and (ii) Mg–E bonding is 12–13 kcal/mol weaker than Hg–E bonding. The trend in the heterolytic BDEs is the same as that for the calculated homolytic BDEs; however, not with regard to the relative magnitude of the Mg–E and Hg–E bonds, which will be discussed below.

The Mg–E bonding strength will increase with increasing ionic character caused by an increasing electronegativity difference  $\Delta\chi$  between Mg and E from Te to S [ $\chi$  values according to Pauling: 1.31 (Mg); 2.58 (S); 2.55 (Se); 2.10 (Te)<sup>56,57</sup>]. The difference in the  $\chi$  values for S and Se is, however, so small (and also the reverse for other electronegativity scales) that one cannot explain the difference

between the BDEs for  $\text{Mg}(\text{SH})_2$  and  $\text{Mg}(\text{SeH})_2$  just by the bond ionicity.

There is a covalent contribution to  $\text{Mg}-\text{E}$  bonding, which depends on the difference between the orbitals involved [ $\text{Mg}^+$ :  $\epsilon(3s) = 15.0$  eV as given by the second ionization potential of  $\text{Mg}$ ;<sup>43</sup>  $\epsilon(3p\sigma) = 13.2$  (S), 12.2 (Se), and 9.8 eV (Te)<sup>22</sup>] and the orbital overlap [the  $3s-3p\sigma$  overlap is larger than the  $3s$  overlap with a diffuse  $5p\sigma(\text{Te})$  orbital]. Hence, the covalent character of  $\text{Mg}-\text{E}$  bonding should also decrease from  $\text{E} = \text{S}$  to  $\text{Te}$ , which is consistent with calculated heterolytic BDEs of 207 (S), 196 (Se), and 192 (Te) kcal/mol and homolytic BDEs of 81 (S), 75 (Se), and 67 (Te) kcal/mol.

Solvation of the ions generated in reaction 5 reduces the endothermicity by 160–180 kcal/mol. However, solvation is less stabilizing for the Se- or Te-containing ions because charge separation in  $\text{H}-\text{E}^-$  and  $\text{HE}-\text{Mg}^+$  is less developed for these ions than for the S-containing ion. The trend in the BDE values is superimposed by the opposite trend in the solvation energies, thus leading to BDE values in water of 29.6, 25.2, and 29.5 kcal/mol (see Table 2).

The calculated BDE values for  $\text{Hg}-\text{E}$  bonds are parallel to those of the  $\text{Mg}-\text{E}$  bonds, with the former being 12–13 kcal/mol larger than the latter in the case of heterolytic dissociation. This is difficult to understand in terms of ionic contributions [ $\chi(\text{Hg}) = 2.0$ , and therefore  $\Delta\chi$  is smaller for  $\text{Hg}-\text{E}$  bonds than for  $\text{Mg}-\text{E}$  bonds] or covalent contributions [ $\text{Hg}^+$ :  $\epsilon(6s) = 18.8$  eV;<sup>43</sup>  $\Delta\epsilon$  for  $\text{Hg}-\text{E}$  bonds is larger, and the orbital overlap is smaller]. There is, however, a third factor: the relativistic contraction of the  $6s(\text{Hg})$  orbital. This contraction leads to a lowering of the  $6s$  orbital energy and larger acceptor ability of the  $\text{Hg}^{2+}$  ion compared to the  $\text{Mg}^{2+}$  ion. In this way, heterolytic BDE values for  $\text{Hg}-\text{E}$  bonds become larger than those for  $\text{Mg}-\text{E}$  bonds. The same effect, however, weakens homolytic  $\text{Hg}-\text{E}$  bonding relative to  $\text{Mg}-\text{E}$  bonding. The relativistic  $6s$  orbital contraction makes the  $6s$  electrons of  $\text{Hg}$  less available for bonding, thus reducing the BDE values for homolytic  $\text{Hg}-\text{E}$  bond cleavage.

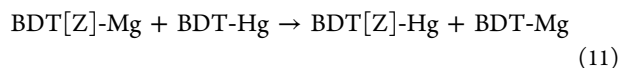
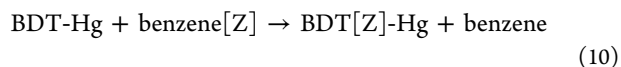
We conclude that the  $\text{M}-\text{E}$  bond strength of both  $\text{Mg}^{\text{II}}$  and  $\text{Hg}^{\text{II}}$  increases from  $\text{Te}$  to  $\text{Se}$  and  $\text{S}$  in the gas phase; however, solvation effects in aqueous solution reverse these trends, yielding different BDE orders for  $\text{Mg}^{\text{II}}$  ( $\text{Se} < \text{S} \approx \text{Te}$ ) and  $\text{Hg}^{\text{II}}$  ( $\text{Se} < \text{S} < \text{Te}$ ).

In Table 1, the NESC energies and free energies for reaction 4 in the gas phase and aqueous solution are listed for variation of  $\text{E}$  in  $\text{BD}(\text{E})-\text{Hg}$  relative to that of  $\text{BD}(\text{E})-\text{Mg}$ . The chalcogenophilicity of  $\text{Hg}^{2+}$  increases from  $\text{S}$  (−98 kcal/mol) to  $\text{Se}$  (−103.4 kcal/mol) and  $\text{Te}$  (−111.6 kcal/mol) by 5 and 8 kcal/mol, respectively, in the gas phase and similar values in aqueous solution. Similarly, somewhat smaller trends are obtained when using  $\text{BDT}(\text{E})\text{T}-\text{Zn}$  rather than  $\text{BDT}(\text{E})\text{T}-\text{Mg}$  as a reference.

In  $\text{BDT}(\text{E})\text{T}-\text{Hg}$ , the almost linear  $\text{E}-\text{Hg}-\text{E}$  unit forces the two amidoethano arms apart according to the calculated  $\text{E}-\text{Hg}$  bond lengths of 2.356 ( $\text{E} = \text{S}$ ), 2.482 (Se), and 2.669 (Te) Å. This, in turn, makes it possible that the  $\text{C}-\text{E}-\text{Hg}$  angle decreases (108.7, 103.4, and 100.2°) and the  $\text{E}-\text{Hg}-\text{E}$  unit becomes more linear (angle  $\text{E}-\text{Hg}-\text{E} = 175.9$ , 176.3, and 176.8°), thus relieving some of the strain of the 14-membered ring. It is noteworthy that this effect will be larger than that indicated by the reaction energy of reaction 4 because for  $\text{BD}(\text{E})-\text{Mg}$  similar, yet smaller, stabilization effects will exist, which partially cancel the  $\text{E}-\text{Hg}$  stabilization effects in the  $\text{Mg}-\text{Hg}$  exchange reaction.

We conclude that the seleno and telluro derivatives of  $\text{BD}(\text{E})$  are more efficient organic tweezer molecules at picking up  $\text{Hg}$  ions from an aqueous solution because of the larger exothermicity of reaction 4 in these cases (see Table 1).

**Nonbonded Interactions with  $\text{Hg}$ .** A change in the interior of the  $\text{BD}(\text{E})-\text{Hg}$  template in positions Y1 and Y2 (see Figure 1) has to consider that the exchange (steric) repulsion between substituents Y1 and Y2 (partly) causes the nonplanarity of the 14-membered ring and determines its inherent ring strain. Any replacement of the H atoms in these positions must be chosen in such a way that an increase in steric repulsion is avoided and instead attractive through-space interactions stabilize the ring. We have chosen reactions 9 and 10 to separate through-space effects from benzene-stabilizing effects and reaction 11 to find out how the  $\text{Mg}-\text{Hg}$  exchange is affected by benzene substitution. As mentioned in section 2, we indicate changes in the substitution pattern of the benzene ring by symbol “[Z]” as in  $\text{BD}(\text{E})[\text{Z}]-\text{M}$ .



where all changes of the benzene ring are denoted by [Z].

The introduction of an F substituent into the Y2 position (see Figure 1) causes stabilization of  $\text{BDT}-\text{Mg}$  by 5.7 kcal/mol relative to benzene. This could be the result of a negatively charged F atom being attracted by a positively charged Mg atom (2.303 Å) or two positively charged H atoms in the Y1 position (distance = 2.064 Å). Clearly, the former is the case, which is also documented by an unusually long C–F bond distance of 1.471 Å compared to a C–F bond length of 1.427 Å in  $\text{BDT}-\text{Hg}$ . The  $\text{Mg}-\text{F}$  distance is comparable to the sum of the ionic radii (2.05 Å), however still much longer than the  $\text{Mg}-\text{F}$  bond length (1.753 Å) in  $\text{MgF}_2$ .<sup>58</sup> There is an electrostatic attraction between the F and Mg atoms, which has the advantage of increasing the F–H distance from the value in  $\text{BDT}-\text{Hg}$  (2.064 Å) to 2.303 Å. This is the reason for the 5.7 kcal/mol stabilization of  $\text{BDT}[\text{F}]-\text{Mg}$ .

Substituting H atoms by F atoms in positions X leads to destabilization of  $\text{BDT}[\text{F}_4]-\text{Mg}$  by 5 kcal/mol, which reveals that steric repulsion between  $\text{F}(\text{Y}2)$  and  $\text{H}(\text{Y}1)$  atoms dominates the stability of  $\text{BDT}[\text{F}_4]-\text{Mg}$ . This is the result of a decrease of the negative charge at  $\text{F}(\text{Y}2)$  caused by withdrawal of the electron density by the other three F substituents of the benzene ring. Accordingly,  $\text{Mg}-\text{F}$  attraction is smaller in  $\text{BDT}[\text{F}_4]-\text{Mg}$  than in  $\text{BDT}[\text{F}]-\text{Mg}$ , as is confirmed by a shorter C–F bond length (1.444 Å) and a longer  $\text{Mg}-\text{F}$  distance (2.141 Å). The  $\text{S}-\text{Mg}-\text{S}$  angle has increased from 114.4 to 149.6°, i.e., to a more linear arrangement, which is an additional indication of a reduced  $\text{Mg}-\text{F}$  attraction.

We conclude that the limited space available in the interior of the 14-membered ring and the amount of steric repulsion between atoms Y1 and Y2 (see Figure 1) determine the stability of compound  $\text{BDT}[\text{Z}]-\text{Mg}$ . This is confirmed for  $\text{Y}2 = \text{Br}$  and  $\text{Y}1 = \text{H}$  (see Table 3), which leads to destabilization of 11 kcal/mol because of the much larger volume of Br compared to H or F [increased steric repulsion between  $\text{H}(\text{Y}1)$  and  $\text{Br}(\text{Y}2)$ ] and the reduced negative charge of Br (decreased  $\text{Br}-\text{Mg}$  attraction). An attempt to solve the space problem in

**Table 3.** NESC/B3LYP and NESC/PCM/B3LYP Energies  $\Delta E$  and  $\Delta G(298)$  (All in kcal/mol) of Dissociation Reactions 9–11

	$\Delta E$			
	reaction 9 (BDT[Z]-M, where M = Mg)		reaction 10 (BDT[Z]-M, where M = Hg)	
	gas	water	gas	water
Y2 = F	-5.7	-4.1	1.4	1.9
X, Y1 = F	5.1	5.1	11.7	12.3
Y2 = Br	11.1	13.0	14.3	15.5
1,3,5-triazine	1.2	1.2	1.8	1.5
	BDT[Z]-M, reaction 11			
	$\Delta E$		$\Delta G(298)$	
	gas	water	gas	water
Y2 = F	7.0	-0.7	6.0	-1.0
X, Y1 = F	6.6	-0.5	7.2	1.3
Y2 = Br	3.2	-0.2	2.6	-0.3
1,3,5-triazine	0.6	0.2	0.4	1.2

position Y2 by replacing the CH group by N as in 1,3,5-triazine does not lead to any change (destabilization by 1.2 kcal/mol) because the N–Mg attraction is too small.

Decreasing the positive charge at the metal atom as in the case of the Hg atom [ $\chi(\text{Hg}) = 2.00$  compared to  $\chi(\text{Mg}) = 1.31$ ] leads to a dominance of destabilizing steric repulsion between Y1 and Y2 over the stabilizing Hg–Y2 attraction. The C–F bond length in BDT[F]-Hg is reduced to 1.427 Å, and the F(Y2)–H(Y1) distance is just 2.064 Å, which is well within the van der Waals distance of 2.67 Å.<sup>43</sup> All BDT[Z]-Hg systems are destabilized, where destabilization is largest for Y2 = Br (14.3 kcal/mol, Table 3).

The energy of the Mg–Hg exchange reaction is equal to the difference  $E(10) - E(9)$  and accordingly should be (slightly or significantly) destabilizing (Table 3). This changes, however, in aqueous solution where *internal solvation* (by Y2) and external solvation of the positively charged metal atom compete. BDT[Z]-Mg is not as externally solvated as BDT[Z]-Hg, thus somewhat compensating for the advantages in internal solvation. All calculated free energy differences  $\Delta G(298)$  in water are either slightly negative or positive. There is a slight advantage of replacing Y2 by F, which is offset by replacing also H(X) by F (see Figure 1). Considering that the actual exchange reaction 4 is strongly exothermic in water (more than 100 kcal/mol), a 1 or 2 kcal/mol change will be insignificant. This can be exploited in the way that the hydrophilicity of the starting material, BDT-Mg, is increased, e.g., by replacing H(X) by F.

**Form of the Precipitate.** It has been repeatedly speculated that the actual precipitate is a polymer of the type  $-(\text{BDT-Hg-BDT-Hg})_n-$  rather than the monomer BDT-Hg. It is beyond the possibilities and the scope of this investigation to calculate possible structures and their energies for such polymers. Nevertheless, we have calculated different conformations of cyclic dimers, which all are more stable in the gas phase or aqueous solution than two monomers according to their energies and enthalpies at 298 K. However, the inclusion of entropy effects leads to positive free energies, indicating that none of the dimers is formed in the gas phase or aqueous solution. We do not consider these calculations to be conclusive because higher oligomers, stabilization of these oligomers by metal ions via keto group coordination, specific solvation effects, and intermolecular interactions between the strands of

polymers may lead to extra stabilization. A detailed investigation of these effects as well as the extension of our studies to higher oligomers is beyond the scope of the current studies.

#### 4. CONCLUSIONS

In this work, we have clarified that the property of chalcogenophilicity of metals such as Mg, Zn, or Hg depends on (i) the oxidation state of the metal, (ii) its coordination sphere, and (iii) environmental factors such as solvation. We find that for the coordination complexes BD(E)-Hg using BD(E)-Mg [or BD(E)-Zn] as a reference, the chalcogenophilicity of  $\text{Hg}^{2+}$  increases in the series  $\text{S} < \text{Se} < \text{Te}$ .

BDT-Hg adopts a  $C_2$ -symmetrical form, which avoids steric repulsion between H(Y1) and H(Y2) atoms (see Figure 1), keeps the amido units nearly planar, however rotated by 30° out of the benzene plane, and has the methylene groups perfectly staggered. The S–Hg–S units are slightly bent toward the center of the 14-membered ring to relieve some of the strain being built up in the ring, which is documented by relatively large bonding angles at the S atoms [108° compared to 94.5 or 92.6 in  $\text{Hg}(\text{SH})_2$  or  $\text{HgSH}^+$ , respectively]. The most stable  $C_s$ -symmetrical form of BDT-Hg is 3.57 kcal/mol higher in energy because of increased ring strain.

In BDT-Hg, Hg is bonded exclusively to the chalcogen atoms. There is no stabilizing interaction with the N atoms (Hg–N distance >4 Å), as was previously speculated.<sup>18</sup>

Experimental investigations to precipitate Hg from water as BDT-Hg compounds have typically started from BDT- $\text{Na}_2$ , i.e., sodium thiolate. We predict on the basis of reliable relativistic calculations that BDT-Mg, i.e., magnesium thiolate, is a much more promising starting product because it already has the 14-membered ring formed, and Mg–Hg exchange does not require any energy.

Chalcogen–mercury binding is stronger than chalcogen–zinc or –magnesium binding because of the strong relativistic 6s orbital contraction that draws the chalcogen charge to the  $\text{Hg}^{2+}$  nucleus.

The increased chalcogenophilicity in the series  $\text{S} < \text{Se} < \text{Te}$  calculated for BD(E)-Hg is a result (among other effects) of decreasing strain in the 14-membered ring, which is due to the increasing length of the unit E–Hg–E and the concomitant decrease of the bond angles at chalcogen atoms E. On the basis of this prediction, we suggest carrying out future removal of mercury from water in the form of a BD(Se)-Hg complex (Figure 3).

We have also shown in this work that the hydrophilicity of the starting product and thereby its solvation by water can be increased by substituting all X atoms in BDT-M (see Figure 1) by F atoms.

There is, however, no possibility of increased mercury bonding by substituting the internal H atoms in positions Y1 and Y2. Strong steric repulsion between any substituent larger than H in the Y2 position (for example, F) and the atoms in the Y1 position excludes this possibility. Only if the metal atom is Mg or any other strongly electropositive atom does electrostatic attraction or even F–M coordination outweigh steric repulsion. However, these internal effects are largely balanced by changes in the external solvation of BDT-M.

On the basis of the results presented in this work, chelating agents more powerful than BDT- $\text{Na}_2$  can be synthesized that can effectively remove Hg from waters. A starting agent such as

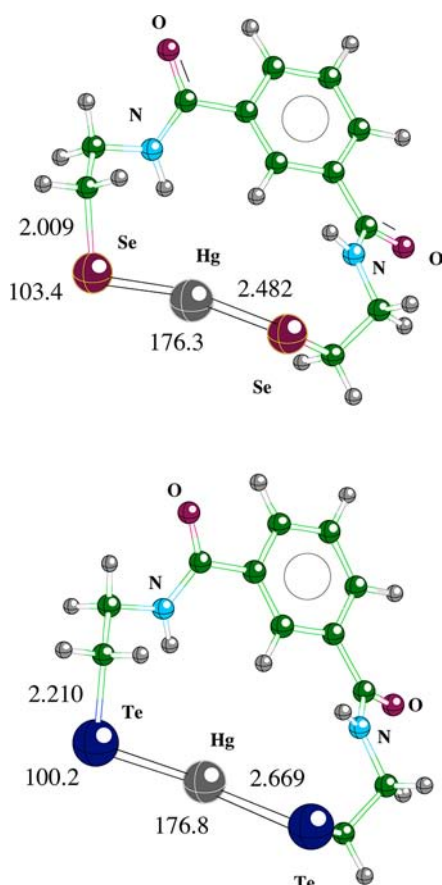


**Figure 3.** NESC/B3LYP geometries of BD(Se)-Hg and BD(Te)-Hg. Distances are in angstroms and angles in degrees.

BD(Se)-Mg with F atoms in the X positions fulfills all criteria outlined in section 3.

## ■ ASSOCIATED CONTENT

### 📄 Supporting Information

Calculated geometries and energies for the stationary points investigated at the NESC/B3LYP/6-31G(d,p) and NESC/CCSD(T)/cc-pVTZ levels of theory. This material is available free of charge via the Internet at <http://pubs.acs.org>.

## ■ AUTHOR INFORMATION

### Corresponding Author

\*E-mail: [dcremer@smu.edu](mailto:dcremer@smu.edu).

### Notes

The authors declare no competing financial interest.

## ■ ACKNOWLEDGMENTS

We thank SMU for providing computational resources.

## ■ REFERENCES

- (1) Clarkson, T. W.; Magos, L. *Crit. Rev. Toxicol.* **2006**, *36*, 609.
- (2) Magos, L.; Clarkson, T. W. *Ann. Clin. Biochem.* **2006**, *43*, 257.
- (3) Wang, Q.; Kim, D.; Dionysou, D. D.; Sorial, G. A.; Timberlake, D. *Environ. Pollut.* **2004**, *131*, 323.
- (4) Kumar, A.; Singh, J. D. *Inorg. Chem.* **2012**, *51*, 772.
- (5) Chen, L.; Yang, L.; Li, H.; Gao, Y.; Deng, D.; Wu, Y.; Ma, L. *Inorg. Chem.* **2011**, *50*, 10028.
- (6) Shi, W.; Li, X.; Ma, H. *Inorg. Chem.* **2010**, *49*, 1206.
- (7) Ho, M.-L.; Chen, K.-Y.; Lee, G.-H.; Chen, Y.-C.; Wang, C.-C.; Lee, J.-F. *Inorg. Chem.* **2009**, *48*, 10304.

- (8) Asaduzzaman, A. M.; Schreckenbach, G. *Inorg. Chem.* **2011**, *50*, 3791.
- (9) Asaduzzaman, A. M.; Schreckenbach, G. *Inorg. Chem.* **2011**, *50*, 2366.
- (10) Melnick, J. G.; Yurkerwich, K.; Parkin, G. *Inorg. Chem.* **2009**, *48*, 6763.
- (11) Melnick, J. G.; Yurkerwich, K.; Parkin, G. *J. Am. Chem. Soc.* **2010**, *132*, 647.
- (12) Melnick, J. G.; Yurkerwich, K.; Buccella, D.; Sattler, W.; Parkin, G. *J. Am. Chem. Soc.* **2008**, *47*, 6421.
- (13) Smith, A. M.; Ne, S. *J. Am. Chem. Soc.* **2011**, *133*, 24.
- (14) Matlock, M. M.; Howerton, B.; Van Aelstyn, M. A.; Nordstrom, F. L.; Atwood, D. A. *Environ. Sci. Technol.* **2002**, *36*, 1636.
- (15) Matlock, M. M.; Howerton, B.; Atwood, D. A. *Water Res.* **2002**, *36*, 4757.
- (16) Matlock, M. M.; Howerton, B.; Atwood, D. A. *Adv. Environ. Res.* **2003**, *7*, 347.
- (17) Matlock, M. M.; Howerton, B.; Van Aelstyn, M. A.; Henke, K. R.; Atwood, D. A. *Water Res.* **2003**, *37*, 579.
- (18) Zaman, K. M.; Blue, L. Y.; Huggins, F. E.; Atwood, D. A. *Environ. Sci. Technol.* **2007**, *46*, 1975.
- (19) Blue, L. Y.; Jana, P.; Atwood, D. A. *Fuel* **2010**, *89*, 1326.
- (20) Hencke, M. K.; Krepps, K. R.; Robertson, J. D.; Atwood, D. A. *Water Res.* **2000**, *34*, 3005.
- (21) Matlock, M. M.; Hencke, K. R.; Atwood, D. A. *J. Hazard Mater.* **2002**, *92*, 129.
- (22) Cremer, D.; Kraka, E.; Filatov, M. *ChemPhysChem* **2008**, *9*, 2510.
- (23) Dyal, K. G. *J. Chem. Phys.* **1997**, *106*, 9618.
- (24) Zou, W.; Filatov, M.; Cremer, D. *Theor. Chem. Acc.* **2011**, *130*, 633.
- (25) Zou, W.; Filatov, M.; Cremer, D. *J. Chem. Phys.* **2011**, *134*, 244117.
- (26) Filatov, M.; Zou, W.; Cremer, D. *J. Phys. Chem. A* **2012**, *116*, 3481.
- (27) Filatov, M.; Zou, W.; Cremer, D. *J. Chem. Phys.* **2012**, *137*, 054113.
- (28) Filatov, M.; Zou, W.; Cremer, D. *J. Chem. Theory Comput.* **2012**, *8*, 875.
- (29) Zou, W.; Filatov, M.; Cremer, D. *J. Chem. Theory Comput.* **2012**, *8*, 2617.
- (30) Zou, W.; Filatov, M.; Cremer, D. *J. Chem. Phys.* **2012**, *137*, 084108.
- (31) Stevens, P. J.; Devlin, F. J.; Chablowski, C. F.; Frisch, M. J. *J. Phys. Chem.* **1994**, *98*, 11623.
- (32) Andrae, D.; Haeussermann, U.; Dolg, M.; Stoll, H.; Preuss, H. *Theor. Chim. Acta* **1990**, *77*, 123.
- (33) Weigend, F.; Ahlrichs, R. *Phys. Chem. Chem. Phys.* **2005**, *7*, 3297.
- (34) Krishnan, R.; Binkley, J. S.; Seeger, R.; Pople, J. A. *J. Chem. Phys.* **1980**, *72*, 650.
- (35) Pantazis, D. A.; Chen, X.-Y.; Landis, C. R.; Neese, F. *J. Chem. Theory Comput.* **2008**, *4*, 908.
- (36) Woon, D. E.; Dunning, T. H., Jr. *J. Chem. Phys.* **1993**, *98*, 1358.
- (37) Wilson, A. K.; Woon, D. E.; Peterson, K. A.; Dunning, T. H., Jr. *J. Chem. Phys.* **1999**, *10*, 76677.
- (38) Visscher, L.; Dyal, K. G. *At. Data Nucl. Data Tables* **1997**, *67*, 207.
- (39) Dyal, K. G.; Fægri, K. *Introduction to Relativistic Quantum Chemistry*; Oxford University Press: Oxford, U.K., 2007.
- (40) Liu, W.; Peng, D. *J. Chem. Phys.* **2009**, *131*, 031104.
- (41) Gabrielse, G.; Hanneke, D.; Kinoshita, T.; Nio, M.; Odom, B. *Phys. Rev. Lett.* **2006**, *97*, 030802.
- (42) Tomasi, J.; Mennucci, B.; Cammi, R. *Chem. Rev.* **2005**, *105*, 2999.
- (43) Lide, D. R. E. *CRC Handbook of Chemistry and Physics on CD-ROM*; CRC Press LLC: Boca Raton, FL, 2000.
- (44) Marcus, Y. *Ion Solvation*; Wiley: Chichester, U.K., 1985.
- (45) Ahlrand, S. *Pure Appl. Chem.* **1990**, *62*, 2077.

- (46) Jiao, D.; King, C.; Grossfield, A.; Darden, T. A.; Ren, P. *J. Phys. Chem. B* **2006**, *110*, 18553.
- (47) Raghavachari, K.; Trucks, K. G. W.; Pople, J. A.; Head-Gordon, M. *Chem. Phys. Lett.* **1989**, *157*, 479.
- (48) Hess, B. A.; Marian, C. M.; Wahlgren, U.; Gropen, O. *Chem. Phys. Lett.* **1996**, *251*, 365.
- (49) Reed, A. E.; Weinstock, R. B.; Weinhold, F. *J. Chem. Phys.* **1985**, *83*, 735.
- (50) Carpenter, J. E.; Weinhold, F. *J. Mol. Struct. (THEOCHEM)* **1988**, *169*, 41.
- (51) Reed, A. E.; Curtiss, L. A.; Weinhold, F. *Chem. Rev.* **1988**, *88*, 899.
- (52) Craig, N. C.; Groner, P.; McKean, D. C. *J. Phys. Chem. A* **2006**, *110*, 7461.
- (53) Kraka, E.; Cremer, D. In *Theoretical Models of Chemical Bonding. The Concept of the Chemical Bond*; Maksic, Z. B., Ed.; Springer Verlag: Heidelberg, 1990; p 453.
- (54) Pyykkö, P.; Straka, M. *Phys. Chem. Chem. Phys.* **2000**, *2*, 2489.
- (55) Eisler, R. *Zinc Hazard to Fish, Wildlife, and Invertebrates: A Synoptic Review*; U.S. Department of the Interior, Fish and Wildlife Service: Laurel, MD, 1993.
- (56) Greenwood, N. N.; Earnshaw, A. *Chemistry of the Elements*; Butterworth-Heinemann: Oxford, U.K., 1997.
- (57) Porterfield, W. W. *Inorganic Chemistry, A Unified Approach*; Academic Press: San Diego, CA, 1993.
- (58) Prascher, B. P.; Woon, D. E.; Peterson, K. A.; Dunning, T. H.; Wilson, A. K. *Theor. Chem. Acc.* **2011**, *128*, 69.